

## The Andy Fund: Progress Report for 2008-2009

Risto A. Kauppinen, M.D., Ph.D.

Director, Biomedical NMR Research Center Research

Professor of Radiology

Dartmouth Medical School

**Project Title: Monitoring treatment response in glioma *in vivo* using functional and metabolic magnetic resonance imaging and positron emission tomography**

We are developing magnetic resonance imaging (MRI) and magnetic resonance spectroscopy (MRS) techniques for pre-surgical assessment of brain tumors as well as for monitoring treatment response. Our goal is to provide non-invasive imaging techniques for brain tumor diagnosis so that the need for diagnostic invasive procedures can be minimized and that responders to given treatment procedure can be identified early on before tumor volume reduction (which often takes place weeks after initiating drug and/or radiation therapies).

In the current project we have used a rat gliosarcoma model, the 9L glioma. This glioma exhibits invasive growth pattern, shares genomic characteristics with human brain tumors and is hypoxic. Thus for imaging purposes the rat glioma model bears great potentials with clinical relevance. Our original proposal was to use MRI and positron emission tomography (PET) in combination to examine tumor hemodynamics and glucose metabolism. Due to low sensitivity and poor spatial resolution of the available micro-PET camera we were forced to modify the protocol and use MRI and  $^1\text{H}$  MRS to address these central variables of tumor function.

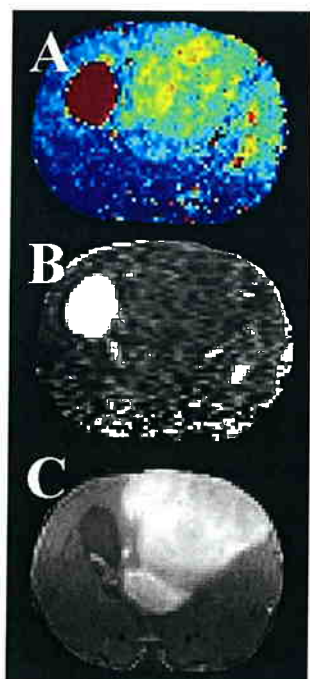


**Fig. 1.** Typical T<sub>2</sub> (A) and D images (B) and a T<sub>1</sub>-weighted, post-contrast image from a 9 glioma rat 25 days after inoculation

A transverse absolute T<sub>2</sub> (data collected with a CPMG sequence), the trace of the diffusion tensor (Dav) images and T<sub>1</sub>-weighted spin echo images after ip injection of gadopentate (0.2 mmol/kg) are shown from a typical 9L glioma bearing rat brain (Fig. 1A-C). It is evident that 9L gliomas exhibit T<sub>2</sub> contrast relative to the brain parenchyma as well as intratumor heterogeneity, and signs for weak Dav contrast to the brain parenchyma.

The presence of low signal intensity zone surrounding the tumor became evident in T<sub>2</sub>-weighted EPI, we termed it as the *tumor rim* (Fig. 2 A and B). This feature has been detected by MRI in other rat gliomas as well and it has been postulated that the rim represents a sub-volume of the tumor where neovascularization is active, in contrast to the core of the tumor where vessels degenerate. From both diagnostic and treatment monitoring point of view it would be attractive to gain deeper understanding of the hemodynamic and metabolic characteristics in these two tumor subvolumes.

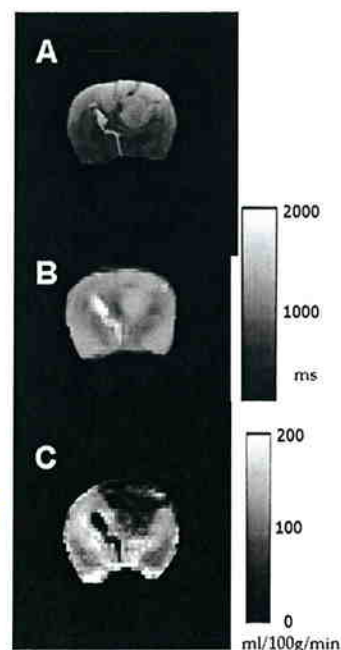


**Fig. 2.** Fast SE image (A), T<sub>1</sub> map (B) and CBF map (C) of a 9L glioma-bearing rat. Gray scale bar next to B gives the scale for T<sub>1</sub> (ms) and that next to C for CBF

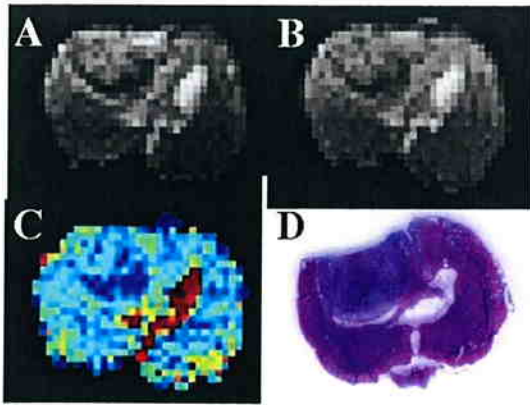


**Fig. 3.** Transverse single (A) and 2-shot (B) SE EPI images from a 9L glioma rat 22 days post-inoculation. A T2 image (C) computed from 2-shot SE EPI data set acquired with 6 TEs. (D) a hematoxylin/eosin stained section through the center of the tumor is shown.

Fig. 3A shows a typical fast-spin echo image (effective TE = 60ms) from a 9L glioma depicting tumor margins with a low signal rim. Fig. 3B and 3C are the T1 and blood flow images, respectively from the same animal. It is evident that the blood flow in the glioma is lower than in the contralateral brain and that there is apparent heterogeneity in the blood flow within the tumor tissue (Fig. 3C). Blood flow data from three 9L bearing rats with comparable size tumors show blood flow values of  $123.0 \pm 58$  and  $51.8 \pm 15.6$  ml/100g/min (mean  $\pm$ SD) in the rim and core, respectively. Blood flow in the contralateral brain was  $179.4 \pm 24.6$  ml/100g/min.

We have determined blood volume and vessel size index (VSI) in 9L gliomas using an iron oxide contrast agent, AMI-227, and to this end, both  $R_2^*$  and  $R_2^*$  were

measured before and after injection of AMI-227. It is well established that the  $\Delta R_2^* / \Delta R_2^*$  ratio is a function of vessel size following injection of intravascular iron oxide-based contrast agents. We found that in the brain parenchyma the  $\Delta R_2^* / \Delta R_2^*$  ratio was  $4.0 \pm 3.4$  and in the tumor rim and core  $9.8 \pm 5.0$  and  $11.0 \pm 10.5$ , respectively. These values transform to VSI in the cortex, tumor rim and core of  $2.23 \pm 2.17$ ,  $18.2 \pm 13.2$ , and  $23.9 \pm 32.8$ , respectively, showing a larger average vessel size in 9L glioma than in the brain parenchyma. Using the  $\Delta R_2^*$  data, the blood volumes in the brain cortex, tumor rim and tumor core were  $1.09 \pm 0.55$ ,  $2.60 \pm 0.66$  and  $2.37 \pm 0.85$  ml/100g, respectively. These measurements show that both tumor rim and core have much enlarged microvasculature with grossly elevated blood volume. Taken together with the blood flow data, it appears that the rim is much better perfused than the core, despite similar microvascular vessel size.

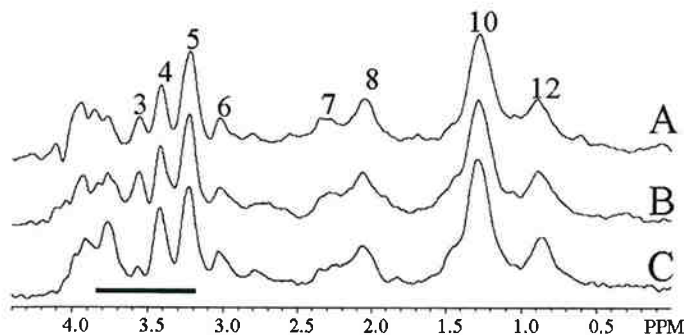


**Fig. 4.** LASER spectra from a voxel ( $3 \times 2.7 \times 3$  mm<sup>3</sup>) acquired before (A) and after (B and C) intraperitoneal D-glucose infusion (2.5 ml of 25% solution) are shown. B was acquired 26 and C 46 minutes after infusion. Peaks are assigned as follows: 3, myo-Inositol+glycine; 4, taurine; 5, CCM; 6, creatine+Phosphocreatine; 7, glutamate; 8, glutamate+Glutamine+ =CH-CH<sub>2</sub>- of lipids; 10, -CH<sub>2</sub>- of lipids and macromolecules + Lactate; 12, -CH<sub>3</sub> of lipids and macromolecules. The horizontal bar indicates the chemical shift region where D-glucose peaks were detected in phantom solution.

<sup>1</sup>H MRS has been used to assess glucose supply and subsequent lactate build-up in brain parenchyma and tumors. Typical spectra (TE=27 ms) from tumor core before (Fig. 4A) and after glucose infusion (Fig. 4B and C) are shown. Glucose resonances appear at 3.25, 3.46, 3.76-3.84 ppm in LASER spectra under these pulsing conditions. Fig 4B and C indicate that peaks in the chemical shift region from 3.8 to 3.4 ppm as well as the broad peak at 1.3 ppm increased in the core following glucose infusion. In two 9L tumor rats the 3.46ppm/Cr ratio increased 2-fold and the 1.3ppm/Cr ratio by 28% by 46

minutes following D-glucose infusion in the tumor core. In the voxel encompassing the rim the respective ratios at this time point were elevated by 117% and 75%. In the contralateral brain the 3.46ppm/Cr ratio was up by 40% only in the first time point, the 1.3ppm/Cr showed no appreciable change during the observation time of 90 min. The ratios of 2.0ppm/Cr did not change in any tissue type during the experiments. These experiments indicate that D-glucose showed up in the  $^1\text{H}$  MRS spectra from all tissue types and that after D-glucose infusion lactate increased only in glioma tissue.

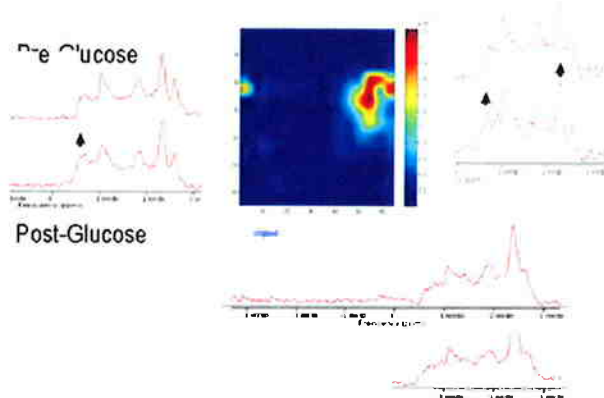


**Fig. 5.** A coronal STEAM CSI image for 1.3 ppm signal of a 9L glioma recorded 44 minutes after infusion of 25% D-glucose (2.5 ml ip.). Spectra from selected voxels are displayed from the acquisitions before and after glucose infusion. B-glucose was 17mM after completion of the STEAM CSI.

We have used chemical shift imaging (CSI) at a spatial resolution of  $4.7 \mu\text{l}$  to tentatively assess anatomical distribution of metabolites in the tumor after D-glucose infusion. A typical CSI of the 1.3ppm resonance is shown (Fig. 5). Selected spectra from tumor voxels are displayed for reference acquired within 44 minutes after D-glucose infusion.

It is evident that in the voxel near the center neither 3.5 ppm/Cr nor 1.3 ppm/Cr ratios change (Fig. 5).

In contrast, in the peripheral areas voxels showing increase in the peaks between 3.7 and 3.5 ppm as well as in 1.3 ppm are observed. Number of tumor voxels in the two 9L rat scanned with CSI before and after D-glucose infusion (2.5 ml 25% D-glucose ip) amounted to 19. There were 6 voxels among the 19 voxels that showed change neither in 1.3ppm/Cr nor 3.46ppm/Cr ratio following glucose infusion (about 30% of CSI-covered tumor in each 9L glioma). The 1.3ppm/Cr and 3.46ppm/Cr ratios increased by more than 30% in 11 and 10 voxels, respectively. Seven of the voxels showed increase in both ratios. These voxels were located outside the center of tumor in both rats. These observations are not surprising in the light of known tumor heterogeneity for cellularity and perfusion.

Our  $^1\text{H}$  MRS and CSI experiments demonstrate that glucose supply, metabolic processing to lactate and lactate retention can be monitored in rat gliomas following infusion of standard D-glucose. This approach deserves to be explored carefully for ability to indicate communication across the tumor vasculature involving facilitated transport across the BBB, uptake by tumor cells and metabolism further to lactate. The present tumor model is anticipated to provide a powerful setting to closely examine the interrelationship between hemodynamic and oxygenation with glucose metabolism to provide pathophysiologically valuable data from biology of gliomas. At the same time, these variables may provide imaging biomarkers for treatment monitoring.

Toward the end of the funding period, attempts to treat 9L gliomas with conventional anti-cancer drugs were taken. To our disappointment, 9L glioma rats did not show appreciable response to cisplatin, etoposide and cyclophosphamide. We currently proceed with investigational agents, including an anti-angiogenic compound.

We are deeply grateful for the award from the Andy Fund, which was crucial to our ability to set up the 9L glioma model as well as to obtain data for two conference proceedings, one manuscript and a RO1 proposal to NIH (pending). Conference Proceedings:

Hekmatyar SK, Liimatainen T, Jerome N, Khan N, Swartz HM and Kauppinen RA (2009)  $^1\text{H}$  MRS detected mobile lipids in rodent gliomas: correlation with EPR determined tumour oxygenation. *Proc Intl Soc Magn Reson Med.* **17**:1016.

Jerome N, Hekmatyar SK and Kauppinen RA (2009) BOLD signal and T2 responses in 9L and F98 gliomas to hypoxic hypoxia. *Proc I*